Available online at www.CivileJournal.org

Civil Engineering Journal

(E-ISSN: 2476-3055; ISSN: 2676-6957)

Vol. 7, No. 12, December, 2021

In-Plane Strengthening of Unreinforced Masonry Walls by Glass Fiber-Reinforced Polyurea

Seung-Hwan Son [1], Jae-Hyoung An [1], Jun-Hyeok Song [1], Yu-Sik Hong [1], Hye-Sook Jang [1], Hee-Chang Eun [1*]

[1] *Department of Architectural Engineering, Kangwon National University, Chuncheon, 24341, Korea.*

Received 28 August 2021; Revised 08 November 2021; Accepted 23 November 2021; Published 01 December 2021

Abstract

Strengthening techniques have been employed in Korea to unreinforced masonry walls (UMWs) for several years to protect them from damage caused by the intermittent occurrence of earthquakes. Polyurea, which has a high tensile strength and elongation rate, can be utilized as a strengthening material to enhance the in-plane strength and ductility of UMWs. Glass fiber-reinforced polyurea (GFRPU) is a composite elastomer manufactured by progressively adding milled glass fiber to polyurea. The purpose of this study is to investigate the enhancement of the in-plane strength and ductility of UMWs using GFRPU, depending on the shape of the GFRPU coating on the wall. Four masonry wall specimens are tested with test variables of the number of strengthening sides and coating shapes. It is illustrated that the GFRPU reinforcement of masonry wall leads to enhanced load-carrying capacity, ductility, and energy absorption. An empirical formula to represent the degree of strengthening effected by GFRPU is proposed in this study.

Keywords: Glass Fiber-Reinforced Poloyurea; In-Plane Load-Carrying Capacity; Retrofit; Energy Absorption Capacity; Unreinforced Masonry Wall.

1. Introduction

Seismic design codes in Korea were first established only in 1988 despite the history of intermittent occurrence of earthquakes. The structures constructed before the codes were established were vulnerable to earthquakes. After the consecutive earthquakes at Kyungju (2016) and Pohang (2017) in South Korea, the necessity of seismic retrofitting in terms of technical and social aspects was raised. One of the noticeable damages reported in the structures was the secondary damage caused by chunks of brick falling on Unreinforced Masonry Walls (UMWs). Secondary damage also included harm to vehicles and adjacent structures.

Several retrofitting techniques have been developed and implemented to enhance the structural and seismic performance of UMWs. Reinforcement should be carried out to enhance the in-plane load-carrying capacity, ductility, and energy absorption. Several strengthening techniques such as the attachment of shotcrete and ferrocement materials to the UMW, grout injection and re-pointing, external steel reinforcement, and fiber-reinforced polymer (FRP) mesh reinforcement have been developed. Wang et al. [1] summarized the strengthening/retrofitting methods based on the fundamental concepts of these methods. Furtado et al. [2] provided a systematic review to investigate the retrofitting

* Corresponding author: heechang@kangwon.ac.kr

http://dx.doi.org/10.28991/cej-2021-03091782

and strengthening strategies of masonry walls. One of the retrofitting methods used to enhance the structural and seismic performance of UMWs is external steel reinforcement using wall ties and steel anchors. The steel jacketing technique of attaching steel members to the UMW can enhance the in-plane lateral strength, ductility, and energy absorption [3]. Darbhanzi et al. [4] investigated the seismic retrofitting of UMWs using two vertical steel ties on either edge of the walls and noticed a significant increase in seismic capacity. The steel jacketing method changes the exterior esthetics, increases the economic burden, breaks the masonry wall, and is prone to tie corrosion.

It has been reported that FRP reinforcement methods for UMWs can improve the strength and ductility of structural members. The FRP mesh is the most widely utilized reinforcement method for improving the in-plane lateral strength of UMWs. Ismail and Ingham [5] considered UMWs reinforced by polymer fiber-reinforced mortar. In particular, they studied the effectiveness of the method of inhibiting the diagonal failure modes. Various variables such as failure mode, stress–strain behavior, shear strength, maximum drift (shear strain), ductility, and number of layers were used, and the shear strength was improved by 114-148% for one-sided reinforcement and 446–481% for two-sided reinforcement. In 2016 [6], in-plane and out-of-plane experiments were performed on the same polymer fiber-reinforced mortar. Most walls demonstrated ductile behavior until they failed, with a 128–136% reinforcement effect.

Papanicolaou et al. [7] conducted an experiment on the effect of the load transfer performance and deformation performance of UMWs under cyclic loads using an external junction grid. The experiment was conducted in two groups: using clay bricks and stone blocks, and 1) in-plane bending with axial force, 2) out-of-plane bending with axial force, and 3) in-plane shear tests were performed. Altin et al. [8] conducted an in-plane repeated load experiment on reinforced concrete frames using carbon-fiber-reinforced polymer (CFRP) strips. The experiment used the width and degree of reinforcement of the CFRP strip as variables. It was reported that as the reinforcement degree of the CFRP strips increased, the lateral resistance and stiffness of the walls increased. El-Diversity et al. [9] conducted an experiment to verify the reinforcement effect of masonry walls reinforced by ferrocement and glass fiber-reinforced polymer (GFRP) complex systems on the in-plane recurrent load. It was noticed that the reinforcement technique increased the ductility and energy absorption capacity by 33% to 85% and the lateral resistance performance by 25% to 32%. Lucchini et al. [10] studied the reinforcement type using steel fiber-reinforced mortar (SFRM) to complete the structural walls. SFRM indicated excellent tensile properties after cracking, so it was bonded to improve the shear resistance of the masonry. Benedetti [11] proposed the strengthening technique to be composed of a glass fiber mesh and fiber reinforced mortar. Haach et al. [12] investigated various parameters to affect the lateral strength of masonry wall. Zhou et al. [13] studied the reinforcement technique of polypropylene bands. Houria et al. [14] and El Malyh et al. [15] presented CFRP reinforcement technique for reinforcing masonry structures.

Polyurea is an elastomer with high deformability, energy absorption capacity, hardness, fracture, and tensile strength. Wu et al. [16] investigated the reinforcing effect based on the polyurea coating thickness and a method for strengthening the UMW against blast loads. The reinforcement technique of UMWs using polyurea reinforced with GFRP was verified experimentally [17]. Further, discrete fiber-reinforced polyurea (DFRP) was introduced for multihazard and/or repair–retrofit applications [18-20]. Glass fiber-reinforced polyurea (GFRPU) used to mix polyurea and milled glass fiber can achieve higher tensile strength while maintaining the other properties of polyurea. The reinforcement effect on concrete beams and columns reinforced by GFRPU [21-23] and the in-plane reinforcement effect of masonry-filled walls [24] were investigated experimentally. In these studies, it was found that the in-plane strength and ductility were significantly enhanced by GFRPU.

In the previous studies, the reinforcing effect of GFRPU to enhance the strength and ductility of reinforced concrete beams and columns was verified. As an extension of these works, this experimental study was conducted to verify the reinforcement effect of masonry walls, which are vulnerable to earthquakes or lateral forces. This study evaluates the degree of improvement in the in-plane load-carrying capacity, ductility, and energy absorption of the UMW caused by GFRPU depending on the shape of the GFRPU coating [21-24]. A 5-mm-thick layer of the composite elastomer GFRPU containing 5% milled glass fiber by weight ratio was sprayed on all specimens. In the experiment, the strength and degree of energy absorption enhancement of the strengthened specimens were compared with the corresponding features of an unreinforced wall. By modifying the Triantafillou and ACI models, this study proposes empirical formulas to describe the improvement in strength caused by GFRPU reinforcement. This experimental study demonstrates that the GFRPU spraying approach has the merit of saving the cost, reducing the construction period, and performing more appropriate reinforcement as compared with other techniques. A flowchart of this study is shown in Figure 1.

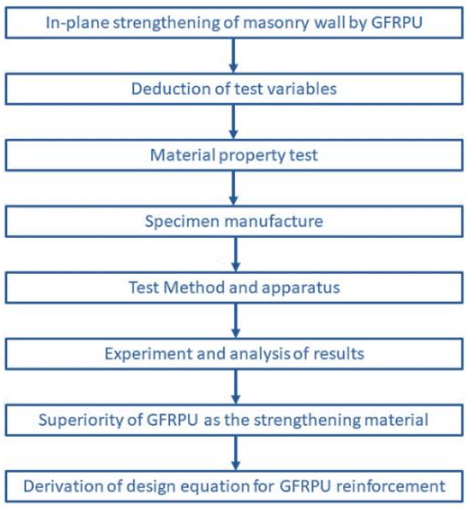

Figure 1. Flowchart of this study

2. Martials and Methods

2.1. Material Properties

GFRPU is a composite elastomer that mixes polyurea with milled glass fibers of length 300 μm. It was reported [24] that the optimum weight ratio of milled glass fiber required to reserve the maximum tensile strength of GFRPU was 5%, and the tensile strength decreased when the weight ratio was higher than 5%. In this experiment GFRPU with 5% weight ratio was used. The milled glass fiber was selected for ease of spraying through a nozzle as compared with chopped glass fiber. Both polyurea and glass fiber were mixed at speeds higher than 500 rpm in a vessel and sprayed at high pressure. The tensile strength of GFRPU was measured based on the Korean Standard KS F 4922, "Polyurea resin waterproofing membrane coating." Thirty specimens were prepared to minimize the deviation in strength caused by nonuniform spraying thickness and dispersion of the glass fiber, and these were tested. The mechanical properties of GFRPU were compared with those of polyurea, as summarized in Table 1. It was noticed that the tensile strength and elastic modulus of GFRPU were enhanced to 36.6% and 44.0%, respectively, owing to the mixture of milled glass fibers, but the elongation rate was slightly decreased to 13.4% with an increase in the amount of glass fiber. GFRPU has sufficient ductility and toughness to obviate abrupt brittle failure despite the decrease in the elongation rate.

The average compressive strength of concrete poured into the concrete frame to enclose the masonry wall depicted in Figure 2 was 26.2 MPa. The average compressive strengths of the concrete bricks utilized in the masonry wall the mortar utilized in the laying bricks were measured as 13.1 and 10.4 MPa, respectively. These values were obtained fro m experiments in accordance with the Korean Standards.

Table 1. Comparison of mechanical properties of polyurea and GFRPU

Property	Polyurea	GFRPU	Rate of increase (%)
Tensile strength (MPa)	22.7	31	36.6
Elastic modulus (MPa)	99.9	143.9	44.0
Elongation rate (%)	418	362	13.4

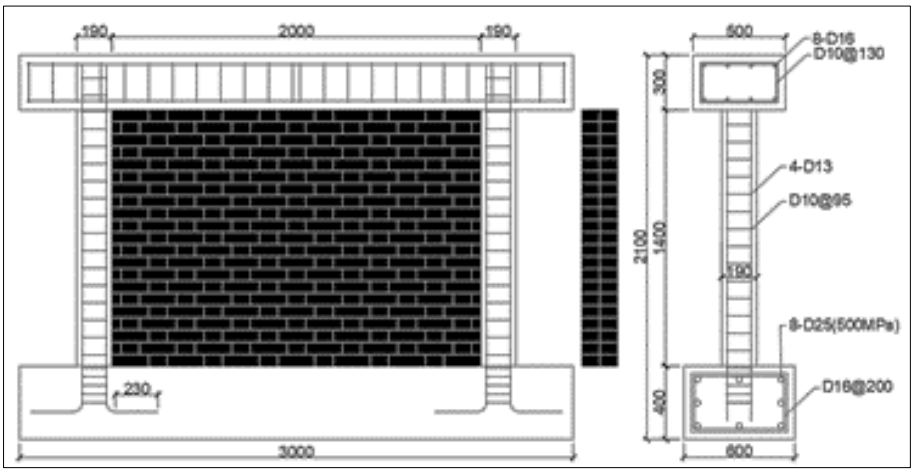

Figure 2. Details of masonry wall and reinforced concrete frame (unit: mm)

2.2. Specimens

The masonry wall specimens were fabricated with a shape ratio of 0.7: length of 2000 mm and height of 1400 mm. The masonry wall was installed in a reinforced concrete frame. The masonry filling wall was built using the 1B stacking method. The upper beam was reinforced by longitudinal bars of 8-D18 and shear reinforcement bars of D10@130. The cross section of the column measured 190 mm × 190 mm, which is the same cross section as the thickness of the 1B stacking of the masonry wall, and is reinforced by longitudinal bars of 4-D13 and lateral reinforcement bars of D10@95. The lower foundation was reinforced by longitudinal bars of 8-D25 and shear reinforcement bars of D16@200. Reinforcing bars of D10, D13, and D18 and D25 with yield strengths of 400 and 500 MPa, respectively, were utilized. The details of the steel reinforcement bars are presented in Figure 2. The concrete in the frame was cast simultaneously, and the experiment was conducted after 28 curing days.

The four masonry wall specimens consisted of an unreinforced specimen and three reinforced specimens. The test variables included the number of strengthening sides using one-sided and two-sided reinforcement and coating shapes. The unreinforced specimen was indicated as "NONE," Arabic numbers 1 and 2 indicated the number of sprayed sides, and "All" and "X" represent the entire and crossing-type coatings, respectively. All the specimens except the unreinforced specimen were bonded and fixed to the concrete frame by 100-mm extended GFRPU spraying from the edges of the masonry wall. GFRPU contained 5% milled glass fiber by weight ratio and a 5-mm-thick layer of it was sprayed on all specimens.

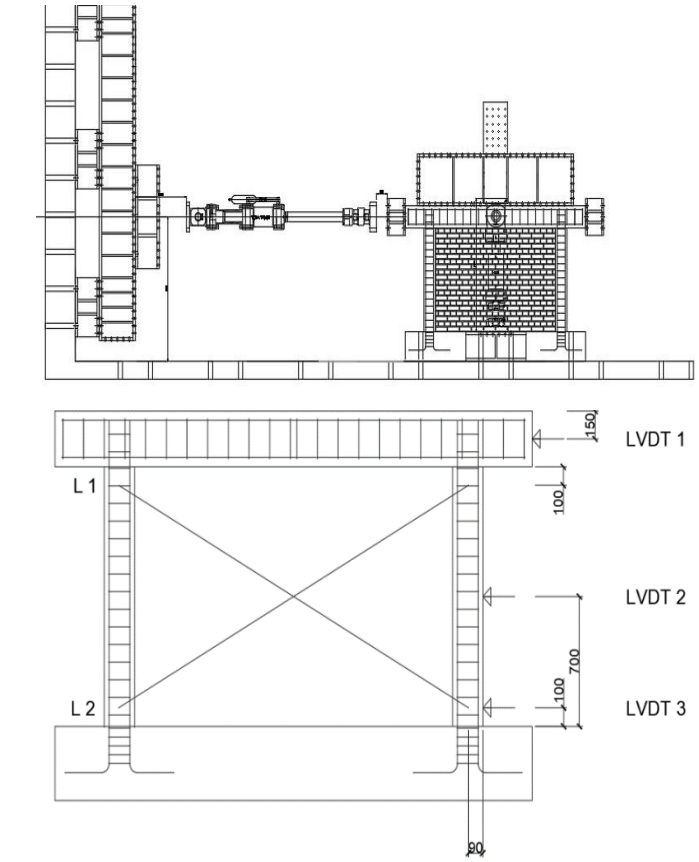

Figure 3. Specimen and loading test apparatus: a) loading system; b) installed sensors; c) photo of specimen and loading system

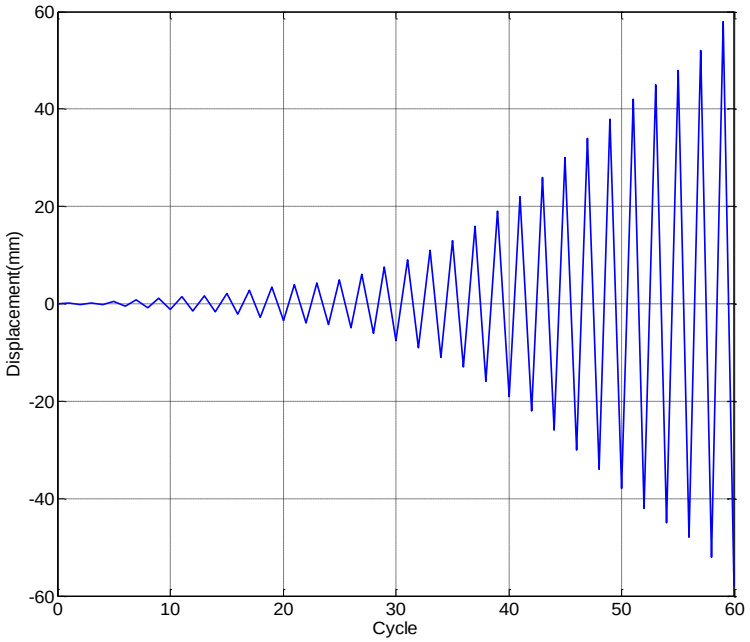

Figure 4. Loading by displacement control

The lower beam of the concrete frame surrounding the masonry wall was fixed to the laboratory floor. The lateral loading in the direction parallel to the upper beam was controlled by displacement without loading in the direction of gravity. The in-plane masonry wall specimen and loading system of the actuator with a capacity of 2000 kN are depicted in Figure 3. The loading was alternatively conducted in the positive and negative directions for identical displacements as they were gradually increased from the initial deformation of 0.4 mm, as depicted in Figure 4. The displacements in the horizontal direction of the specimens were measured using three linear variable displacement transducers (LVDTs), and two additional LVDTs measured the displacements in the diagonal direction.

3. Failure Modes

Initial cracks originated from the diagonal cracks at the wall corners. They gradually developed in the middle of the wall with an increase in the lateral load, and the crack width increased. More explicit diagonal cracks were seen in the unreinforced specimen as compared with the GFRPU specimens (Figures 5 and 6) because the specimens strengthened by GFRPU controlled the crack development caused by the tensile capacity of GFRPU. The initial cracks in all the specimens appeared in the displacement range of 0.2–0.8 mm, as presented in Table 2.

Table 2. Load and displacement at major stages

Specimens	Initial crack		Positive direction		Negative direction	
	Load (kN)	Displacement (mm)	First peak load/Second peak load (kN)	Displacement at first/second peak load (mm)	First peak load/Second peak load (kN)	Displacement at first/second peak load (mm)
NONE	-70	-0.2	159.7/174.57	3.41/14.58	158.3/179.11	3.44/15.78
1-ALL	117	+0.8	207.94/200.4	2.76/10.87	174.25/149.4	3.03/10.3
2_ALL	+122	+0.8	227.15/200.3	7.11/12.82	210.19/202.7	4.91/7.17
1-X	-111	-0.8	198.9/199.65	3.79/10.99	181.8/223.64	5.02/21.99

(a) **(b)**

(c) **(d)**

Figure 5. Photos of failed specimens after experiments: (a) NONE, (b) 1-All, (c) 2-All, (d) 1-X

FEMA 273 [25] and FEMA 306 [26] reported that a masonry wall subjected to an in-plane load fails by rocking, toe crushing, sliding, and diagonal tension. Diagonal tension and mortar cracks were evident in all the specimens. Mortar cracks at the bed joints were found in all the specimens owing to the low bond strength between the bricks. The unreinforced NONE specimen indicates tension cracks as well as mortar cracks along the diagonal direction. The crack patterns exhibited a failure mode similar to that of pure shear.

The crack development of the other reinforced specimens was delayed by GFRPU strengthening owing to the limited development of diagonal tension cracks. The shear and bond-resisting capacity of the mortar between the bricks were also enhanced by the GFRPU reinforcement. This indicates that the GFRPU reinforcement enhances the bond strength between the mortar and the bricks and the mechanical capacity of the specimens. The reinforced specimens failed, as indicated by mortar cracks in the longitudinal directions except at the wall corners. It was estimated that the cracks were caused by mortar sliding between the bricks owing to the low bond strength. The strengthening effect was established as the cracks of the GFRPU-reinforced specimen occurred at a point higher than the peak load of the unreinforced specimen. Despite the higher lateral load, the peel of GFRPU and the dropping of bricks were rarely noticed. The failure modes indicated that GFRPU could control the crack patterns and failure modes based on the degree of reinforcement.

4. Load-Displacement Curves

The validity of the GFRPU reinforcement technique was investigated by comparing the load–displacement curves based on the experimental parameters. The lateral displacement was measured using LVDTs at the top of the concrete frame, as illustrated in Figure 3(b). The spraying was performed manually by technical experts. However, it was not possible to sustain uniform dispersion of the glass fiber and coating thickness of GFRPU during spraying. The locally vulnerable region could be embedded in the sprayed wall owing to the inaccurate operation. The inaccurate spraying affected the results of the experiment.

The specimens resisted the lateral load owing to the masonry wall and concrete frame. The load–displacement hysteresis curves depicted in Figure 7, including the peak load-carrying capacity, ductility, and energy absorption of the specimens, exhibited slightly different shapes depending on the degree of strengthening. The maximum load-carrying capacity and corresponding displacements are listed in Table 2. GFRPU strengthening leads to an enhanced peak load-carrying capacity. It is illustrated that the first peak load was enhanced with the increase in the constraint capacity caused by GFRPU and its range was based on the degree of control of the expansion in the out-of-plane direction of the wall. The first peak load is a meaningful value for maximizing the strengthening effect caused by GFRPU. The load-carrying capacity of the unreinforced specimen NONE deteriorated abruptly, and the lateral load-resisting capacity at the post-peak load was sustained by the concrete frame. After the other reinforced specimens except the 2-All specimens reached the first peak load, abrupt deterioration of the lateral load-resisting capacity was noticed with damage to the masonry wall, such as diagonal cracks and mortar cracks. It is estimated that a part of the load-carrying capacity of the masonry wall disappeared at this time. Subsequently, the lateral load was supported by the concrete frame and gradually increased, and it reached the second peak load. The first peak load of 2-All specimen represents the peak load because the masonry wall and concrete frame behave monolithically as the masonry wall was constrained by two-sided reinforcement. The two-sided reinforcement technique is the most effective in strengthening the UMW in the in-plane direction because it constrains the lateral expansion.

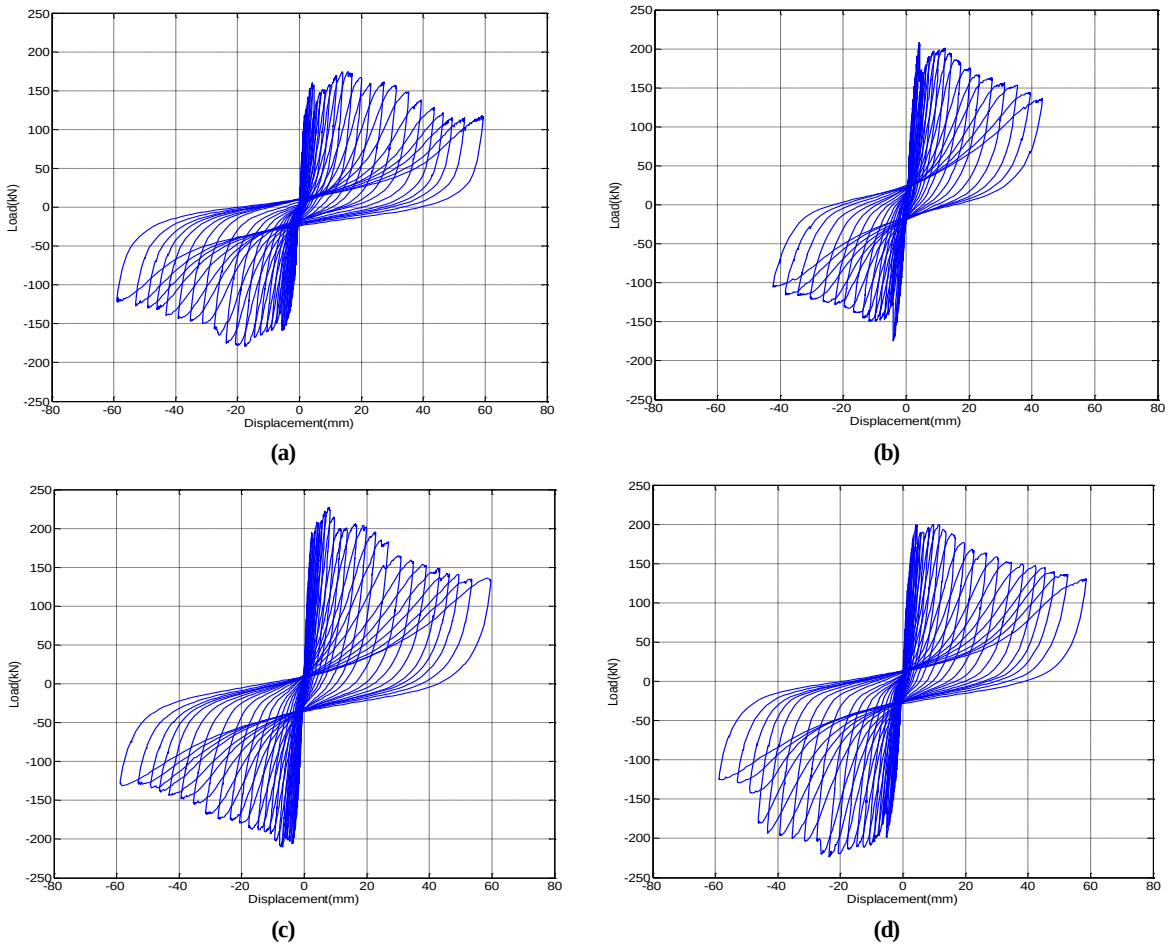

Figure 7. Load-displacement curves: (a) NONE, (b) 1-All, (c) 2-All, (d) 1-X

After the second peak load was reached, the specimens exhibited ductile behavior owing to the mechanical properties of the GFRPU material. However, most of the load-resisting capacity was sustained by the concrete column as against the behavior at the post-peak load. In the plots, the improvement in ductility capacity caused by the GFRPU is explained by the difference between the load–displacement curves of the unreinforced and GFRPU-reinforced specimens. It was also noticed that the range of ductility capacity was based on the degree of strengthening. Under the lateral load in the negative direction, the load–displacement curves display a slightly different aspect from that in the positive direction. The 1-All specimens exhibited a lower ductility capacity in the negative direction as compared with the unreinforced specimens. The 1-X specimens exhibited a more ductile capacity as compared with the 2-All specimens. This observation is attributed to the displacements caused by sliding owing to the closure and opening of the cracks during loading in alternative directions after reaching the peak load in the positive direction.

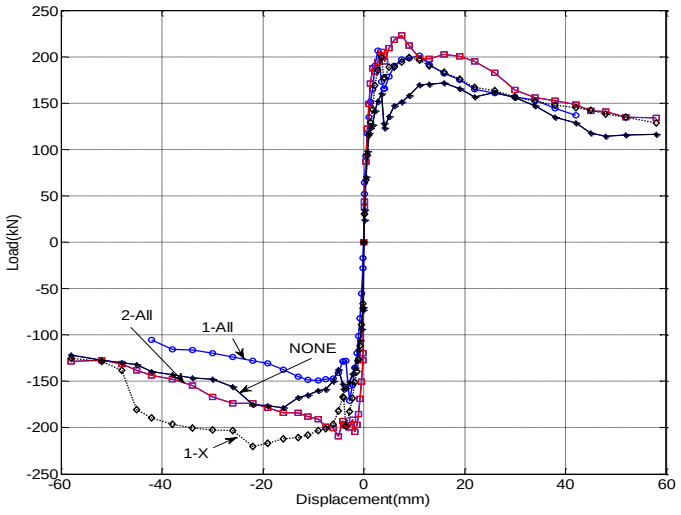

Figure 8. Comparison of load-displacement curves

5. Energy Absorption Capacity

Figure 7 presents the curves plotted between the repeated lateral loads and the corresponding displacements. Figure 7 presents the load–displacement curves that connect the peak loads in the positive and negative directions of each cycle. As depicted in Figures 7 and 8, the energy absorption capacity improved with an increase in the degree of reinforcement, which is caused by the high elongation rate, a mechanical property of the polyurea material. The energy absorption capacity for a displacement of 42 mm in the positive and negative directions is quantitatively compared in Table 3, through this analysis, as depicted in Figure 8. The absorption capacity improved with the GFRPU reinforcement. The increase rates in percentage with respect to that in the unreinforced specimen were 17%, 43%, and 34% for the 1-All, 2-All, and 1-X specimens, respectively. It was noticed that the rate of increase in the absorption energy of the 1-All specimen was underestimated, similar to the peak load, because of the error in operation caused by the non-uniform spraying thickness. The GFRPU was dispersed and abruptly stuck in the prescribed area through a small nozzle hole owing to the high-pressure spraying. The area in which it was stuck was larger than the nozzle hole, which caused the 1-X specimen to be unexpectedly stuck in an area similar to the 1-All specimen. Thus, the load-resisting and energy absorption capacities of the 1-X specimens were similar to or greater than those of the 1-All specimens.

Table 3. Comparison of mechanical properties of polyurea and GFRPU

Specimen	Energy absorption capacity (kN-m)	Improved rate (%)
NONE	30.0	-
1-All	35.2	17
2-All	42.9	43
1-X	40.2	34

6. Derivation of Formula to Describe the GFRPU Reinforcement

By modifying the Triantafillou [7] and AC125 [25, 26] models, this study proposed formulas to describe the degree of strengthening caused by GFRPU. It is not practical to construct a two-sided reinforcement using GFRPU, and the X-type reinforcement is rarely differentiated from the one-sided reinforcement of the wall when considering the construction and the experimental results. Thus, one-sided spraying is a universal method in terms of strength, construction, and economy. The strengthening degree can be predicted based on the difference in load between the peak load-carrying capacities of the unreinforced and 1-All specimens.

(1) Modification of Triantafillou model

The in-plane load-carrying capacity P is determined by adding the shear strengths of the UMW and GFRPU reinforcement as follows:

$$P = F_m + F_G \tag{1}$$

where F_m denotes the shear strength of the UMW and takes the minimum value of the shear strength calculated by the four failure modes of rocking, toe crushing, sliding, and diagonal tension failure specified in the Korean code [27]. F_G represents the shear strength carried by the GFRPU and is derived using the experimental results. It is expressed as

$$F_G = \propto \gamma\lambda\rho_h E_G \epsilon_{max,G} tL \tag{2}$$

where $\propto$: denotes the shear reinforcement factor (= 0.0093 for GFRPU with a weight ratio of 5%); γ: = 1 in the case of one-sided reinforcement and 1.5 in the case of two-sided reinforcement; λ: is the ratio of the sprayed area with respect to the entire wall area; ρ_h: is the reinforcement ratio in the horizontal direction; E_G: is the elastic modulus of GFRPU; $\epsilon_{max,G}$: is the elongation rate at the point of fracture of GFRPU; t: is the thickness of the masonry wall; and L: is the length of the masonry wall. The material properties of the elastic modulus and elongation rate of GFRPU at the point of fracture were determined by a material test.

(2) Modification of AC125 Model

This model was presented in a report presented by the International Code Council (ICC). It predicted the shear strength to strengthen the UMW using one-sided FRP. The modification of the model caused by the GFRPU reinforcement is expressed as follows:

$$F_G = 0.75\gamma\lambda\rho_h f_j tL \tag{3}$$

where f_j represents the load-resisting capacity in the axial direction expressed as

$$f_j = \beta E_G \leq 0.75 f_{G,u} \tag{4}$$

$f_{G,u}$ represents the ultimate tensile strength, and β represents the shear reinforcement factor and was selected as 0.0447 for GFRPU with a 5% weight ratio from the experimental results.

Using Equations 2 and 3, the load-resisting capacity of GFRPU is listed in Table 4. Thus, it is illustrated that the formulae predict the load-resisting capacity accurately.

Table 4. Comparison of mechanical properties of polyurea and GFRPU

Specimen	Experiment (kN)	Modified Triantafillou (kN)	Modified AC125 (kN)
NONE	159.7	159.7	159.7
1-All	207.94	208.12	207.9
2-All	227.15	232.3	232.0
1-X	198.9	193.6	193.4

7. Conclusion

In this study, the strengthening effect was investigated depending on the coating shape of GFRPU used to mix polyurea with milled glass fiber. The material property of GFRPU, which has a high tensile strength and elongation rate, improves the in-plane load-carrying capacity and ductility of the UMW. The in-plane strength of the GFRPU reinforcement was enhanced by lateral confinement of the masonry wall, which improved the shear-resisting capacity of the masonry wall. The ductile capacity of the GFRPU reinforcement can prevent secondary damage caused by the falling of bricks. Despite excellent material properties, because it is not easy to ensure the uniform dispersion of glass fiber and coating thickness during spraying, it was illustrated that the reinforced masonry wall could fail at a lower load than the expected load-carrying capacity. The experiment indicated that the one-sided reinforcement of the masonry wall was excellent in terms of economic and constructional aspects. By modifying the Triantafillou and AC125 models, this study proposed formulas to describe the degree of strengthening caused by one-sided GFRPU. In future studies, the relationships among strength, ductility, and energy absorption of masonry walls will be evaluated based on the thickness of the coating.

8. Declarations

8.1. Author Contributions

Conceptualization, H.C.E.; methodology, S.H.S.; software, J.H.A.; validation, S.H.S., H.S.J. and Y.S.H.; formal analysis, J.H.A.; investigation, S.H.S.; resources, Y.S.H.; data curation, S.H.S.; writing—original draft preparation, S.H.S.; writing—review and editing, H.C.E.; visualization, J.H.S.; supervision, H.C.E.; project administration, H.C.E.; funding acquisition, H.C.E. All authors have read and agreed to the published version of the manuscript.

8.2. Data Availability Statement

The data presented in this study are available in article.

8.3. Funding

The authors received no financial support for the research, authorship, and/or publication of this article.

8.4. Conflicts of Interest

The authors declare no conflict of interest.

9. References

[1] Wang, Chuanlin, Vasilis Sarhosis, and Nikolaos Nikitas. “Strengthening/Retrofitting Techniques on Unreinforced Masonry Structure/Element Subjected to Seismic Loads: A Literature Review.” The Open Construction and Building Technology Journal 12, no. 1 (2018): 251–68. doi:10.2174/1874836801812010251.

[2] Furtado, André, Hugo Rodrigues, António Arêde, and Humberto Varum. “Experimental Tests on Strengthening Strategies for Masonry Infill Walls: A Literature Review.” Construction and Building Materials 263 (2020). doi:10.1016/j.conbuildmat.2020.120520.

[3] Rai, Durgesh C., and Subhash C. Goel. “Seismic Strengthening of Unreinforced Masonry Piers with Steel Elements.” In Earthquake Spectra, 12:845–62. Calgary, Canada, 1996. doi:10.1193/1.1585913.

[4] Darbhanzi, A., M. S. Marefat, and M. Khanmohammadi. “Investigation of In-Plane Seismic Retrofit of Unreinforced Masonry Walls by Means of Vertical Steel Ties.” Construction and Building Materials 52 (2014): 122–29. doi:10.1016/j.conbuildmat.2013.11.020.

[5] Ismail, Najif, and Jason M. Ingham. "Polymer Textiles as a Retrofit Material for Masonry Walls." Proceedings of the Institution of Civil Engineers: Structures and Buildings 167, no. 1 (2014): 15–25. doi:10.1680/stbu.11.00084.

[6] Ismail, Najif, and Jason M. Ingham. "In-Plane and out-of-Plane Testing of Unreinforced Masonry Walls Strengthened Using Polymer Textile Reinforced Mortar." Engineering Structures 118, no. 1 (2016): 167–77. doi:10.1016/j.engstruct.2016.03.041.

[7] Papanicolaou, Catherine, Thanasis Triantafillou, and Maria Lekka. "Externally Bonded Grids as Strengthening and Seismic Retrofitting Materials of Masonry Panels." Construction and Building Materials 25, no. 2 (2011): 504–14. doi:10.1016/j.conbuildmat.2010.07.018.

[8] Altin, Sinan, Özgür Anil, M. Emin Kara, and Mustafa Kaya. "An Experimental Study on Strengthening of Masonry Infilled RC Frames Using Diagonal CFRP Strips." Composites Part B: Engineering 39, no. 4 (2008): 680–93. doi:10.1016/j.compositesb.2007.06.001.

[9] El-Diasity, Mosaad, Hussein Okail, Osama Kamal, and Mohamed Said. "Structural Performance of Confined Masonry Walls Retrofitted Using Ferrocement and GFRP under In-Plane Cyclic Loading." Engineering Structures 94 (2015): 54–69. doi:10.1016/j.engstruct.2015.03.035.

[10] Lucchini, Sara S., Luca Facconi, Fausto Minelli, and Giovanni Plizzari. "Retrofitting Unreinforced Masonry by Steel Fiber Reinforced Mortar Coating: Uniaxial and Diagonal Compression Tests." Materials and Structures/Materiaux et Constructions 53, no. 6 (2020): 1–22. doi:10.1617/s11527-020-01574-w.

[11] Triantafillou, Thanasis C. "Strengthening of Masonry Structures Using Epoxy-Bonded FRP Laminates." Journal of Composites for Construction 2, no. 2 (1998): 96–104. doi:10.1061/(asce)1090-0268(1998)2:2(96).

[12] Bae, Baek-Il, Hyo-Jin Yun, Chang-Sik Choi, and Hyun-Ki Choi. "Evaluation of Shear Strength of Unreinforced Masonry Walls Retrofitted by Fiber Reinforced Polymer Sheet." Journal of the Korea Concrete Institute 24, no. 3 (2012): 305–13. doi:10.4334/jkci.2012.24.3.305.

[13] Babaeidarabad, Saman, Francisco De Caso, and Antonio Nanni. "URM Walls Strengthened with Fabric-Reinforced Cementitious Matrix Composite Subjected to Diagonal Compression." Journal of Composites for Construction 18, no. 2 (2014): 04013045. doi:10.1061/(asce)cc.1943-5614.0000441.

[14] Faella, Ciro, Enzo Martinelli, Emidio Nigro, and Sergio Paciello. "Shear Capacity of Masonry Walls Externally Strengthened by a Cement-Based Composite Material: An Experimental Campaign." Construction and Building Materials 24, no. 1 (2010): 84–93. doi:10.1016/j.conbuildmat.2009.08.019.

[15] Benedetti, Andrea. "In Plane Behaviour of Masonry Walls Reinforced with Mortar Coatings and Fibre Meshes." International Journal of Architectural Heritage 13, no. 7 (2019): 1029–41. doi:10.1080/15583058.2019.1618972.

[16] Haach, Vladimir G., Graça Vasconcelos, and Paulo B. Lourenço. "Parametrical Study of Masonry Walls Subjected to In-Plane Loading through Numerical Modeling." Engineering Structures, 2011. doi:10.1016/j.engstruct.2011.01.015.

[17] Zhou, Qiang, Lingyu Yang, and Wenyang Zhao. "Experimental Analysis of Seismic Performance of Masonry Shear Wall Reinforced with PP-Band Mesh and Plastering Mortar under In-Plane Cyclic Loading." In Advances in Civil Engineering, Vol. 2020, 2020. doi:10.1155/2020/4015790.

[18] Hernoune, Houria, Benchaa Benabed, Antonios Kanellopoulos, Alaa Hussein Al-Zuhairi, and Abdelhamid Guettala. "Experimental and Numerical Study of Behaviour of Reinforced Masonry Walls with NSM CFRP Strips Subjected to Combined Loads." Buildings 10, no. 6 (2020). doi:10.3390/BUILDINGS10060103.

[19] Elmalyh, Sanaa, Azzeddine Bouyahyaoui, Toufik Cherradi, Ancuta Rotaru, and Petru Mihai. "In-Plane Shear Behavior of Unreinforced Masonry Walls Strengthened with Fiber Reinforced Polymer Composites." Advances in Science, Technology and Engineering Systems 5, no. 2 (2020): 360–67. doi:10.25046/AJ050247.

[20] Augenti, N., F. Parisi, A. Prota, and G. Manfredi. "In-Plane Lateral Response of a Full-Scale Masonry Subassemblage with and without an Inorganic Matrix-Grid Strengthening System." Journal of Composites for Construction 15, no. 4 (2011): 578–90. doi:10.1061/(asce)cc.1943-5614.0000193.

[21] Yu, P, and P F Silva. Strengthening of Infill Masonry Walls Using Bondo Grids with Polyurea. Center for Repair of Bridges and Buildings, (2005).

[22] Carey, N. L., and J. J. Myers. "Discrete Fiber Reinforced Polymer Systems for Repair of Concrete Structures: Polyurea-Fiber Characterization Results." American Concrete Institute, ACI Special Publication 1, no. 275 SP (2011): 275–88.

[23] Carey, N. L., and J. J. Myers. "Full Scale Blast Testing of Hybrid Barrier Systems." In American Concrete Institute, ACI Special Publication. American Concrete Institute, (2010): 152–70.

[24] Greene, C. E. "Compressive behavior of concrete cylinders strengthened with a discrete fiber reinforced polymer system." M.S. Thesis (2010). Missouri Univ. of Science and Technology, Rolla, MO.

[25] Song, Jun Hyeok, Eun Taik Lee, and Hee Chang Eun. "A Study on the Improvement of Structural Performance by Glass Fiber-Reinforced Polyurea (GFRPU) Reinforcement." In Advances in Civil Engineering, Vol. 2019, 2019. doi:10.1155/2019/2818219.

[26] Song, Jun Hyuk, Eun Taik Lee, Hee Chang Eun, and Charis Apostolopoulos. "A Study on the Strengthening Performance of Concrete Beam by Fiber-Reinforced Polyurea (FRPU) Reinforcement." In Advances in Civil Engineering, Vol. 2020, 2020. doi:10.1155/2020/6967845.

[27] Song, Jun Hyeok, Eun Taik Lee, and Hee Chang Eun. "Shear Strength of Reinforced Concrete Columns Retrofitted by Glass Fiber Reinforced Polyurea." Civil Engineering Journal (Iran) 6, no. 10 (2020): 1852–63. doi:10.28991/cej-2020-03091587.

[28] Son, S H. A Study on In-Plane Strengthening Effect of Masonry Wall by Composite Material of Milled Glass Fiber and Polyurea. Kangwon National University, (2021).

[29] FEMA 273, Nehrp Guidelines for the Seismic Rehabilitation of Buildings (1997).

[30] ATC. "FEMA 307. Evaluation of Earthquake Damaged Concrete and Masonry Wall Buildings. Technical Resources." Management, (1998).

[31] Corporation, Korea Facilities Safety. "Seismic Performance Evaluation Guidelines for Existing Facilities", Buildings, (2019).